Massive volcanism, evaporite deposition, and the chemical evolution of the Early Cretaceous ocean

Jennifer V. Mills, Maya L. Gomes, Brian Kristall, Bradley B. Sageman, Andrew D. Jacobson, and Matthew T. Hurtgen*
Department of Earth and Planetary Sciences, Northwestern University, 2145 Sheridan Road, Evanston, Illinois 60208, USA

ABSTRACT

Early Cretaceous (145–100 Ma) rocks record a ~5‰ negative shift in the sulfur isotope composition of marine sulfate, the largest shift observed over the past 130 m.y. Two hypotheses have been proposed to explain this shift: (1) massive evaporite deposition associated with rifting during opening of the South Atlantic and (2) increased inputs of volcanically derived sulfur due to eruption of large igneous provinces. Each process produces a very different impact on marine sulfate concentrations, which in turn affects several biogeochemical phenomena that regulate the global carbon cycle and climate. Here we present sulfur isotope data from Resolution Guyot, Mid-Pacific Mountains (North Pacific Ocean), that track sympathetically with strontium isotope records through the ~5‰ negative sulfur isotope shift. We employ a linked sulfur-strontium isotope mass-balance model to identify the mechanisms driving the sulfur isotope evolution of the Cretaceous ocean. The model only reproduces the coupled negative sulfur and strontium isotope shifts when both hydrothermal and weathering fluxes increase. Our results indicate that marine sulfate concentrations increased significantly during the negative sulfur isotope shift and that enhanced hydrothermal and weathering input fluxes to the ocean played a dominant role in regulating the marine sulfur cycle and CO_2 exchange in the atmosphere-ocean system during this interval of rapid biogeochemical change.

INTRODUCTION

The sulfate content of the ocean plays an important role in regulating the global carbon cycle and the chemical composition of the ocean-atmosphere system. For example, in the present sulfate-rich ocean, microbial sulfate reduction (MSR) remineralizes as much as 50% of the organic matter in coastal marine sediments (Jørgensen, 1982) and affects phosphorus recycling efficiency and therefore marine primary productivity (Ingall et al., 1993; Van Cappellen and Ingall, 1996; Adams et al., 2010). Moreover, MSR increases carbonate alkalinity via bicarbonate production, which in turn affects the partitioning of CO_2 between the atmosphere and ocean (Zeebe and Wolf-Gladrow, 2001). However, marine sulfate concentrations have varied considerably over geologic time (Lowenstein et al., 2001), affecting the marine carbon cycle, the evolution of Earth's climate system, and the long-term redox balance of the ocean-atmosphere system.

The relative importance of marine sulfur inputs and outputs through time can be tracked in part by reconstructing the S isotope composition of sulfate phases (i.e., barite, calcium sulfate, and carbonate-associated sulfate) preserved in marine sedimentary rocks. The S isotope composition of marine sulfate ($\delta^{34}S_{sulfate}$) represents a balance between the input of ^{34}S-depleted S from riverine (continental weathering) and hydrothermal sources and the removal of ^{34}S-depleted S via MSR and associated pyrite burial (Canfield, 2001).

An ~5‰ negative excursion extending from ca. 126 to 100 Ma represents the most distinguishing feature of the $\delta^{34}S_{sulfate}$ record spanning the past 130 m.y. (Paytan et al., 2004; Fig. 1). While original interpretations of
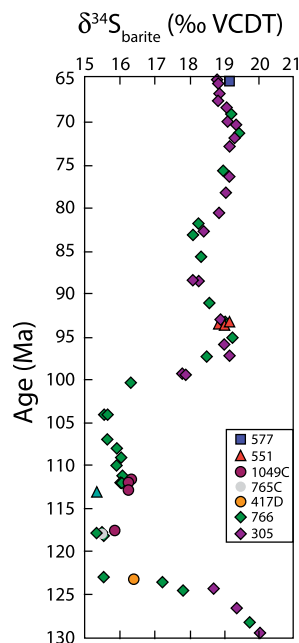

$\delta^{34}S_{barite}$ (‰ VCDT)

Figure 1. The sulfur isotope composition of Cretaceous marine barite ($\delta^{34}S_{sulfate}$, ‰ VCDT [Vienna Canyon Diablo troilite]; Paytan et al., 2004) plotted versus time (Prokoph et al., 2008). Numbers next to colored symbols represent Ocean Drilling Program sites.

this event implicated a combination of increased hydrothermal and weathering inputs and decreased pyrite burial rates as possible triggers (Paytan et al., 2004), more recent work postulates that increased evaporite deposition (calcium sulfate) associated with the opening of the South Atlantic during this time dramatically lowered marine sulfate concentrations and facilitated a drop in relative pyrite burial rates (Wortmann and Chernyavsky, 2007; Wortmann and Paytan, 2012). Either of these processes operating in isolation could account for the negative $\delta^{34}S_{sulfate}$ excursion. However, each has a very different impact on marine sulfate concentrations: increased volcanism and continental weathering rates increase sulfate delivery to the ocean, whereas evaporite deposition removes it during calcium sulfate precipitation. Although there is geologic evidence for both massive evaporite deposition (Hay et al., 2006; Davison, 2007; Chaboureau et al., 2013) and extensive volcanism due to the formation of several large igneous provinces (LIPs) during the Early Cretaceous (Chandler et al., 2012; Mills et al., 2014), the relative importance of these factors in regulating marine sulfate levels and attendant biogeochemical change remains unconstrained.

The Cretaceous Period (ca. 145–65 Ma) is also punctuated by several ocean anoxic events (OAEs), short-term (<1 m.y.) intervals of carbon cycle disruption during which massive amounts of organic carbon were buried in marine sediments (Schlanger and Jenkyns, 1976). OAE1a occurred at ca. 125 Ma (Ogg et al., 2012), although its temporal relationship with the negative $\delta^{34}S_{sulfate}$ shift has not been documented unambiguously (Gomes et al., 2016). Given the strong coupling between the geochemical cycles of carbon and sulfur, improved understanding of how ocean chemistry and sulfate concentrations evolved over this period could provide insight into the factors that conditioned the oceans for carbon cycle instability (Wortmann and Chernyavsky, 2007; Adams et al., 2010; Gomes et al., 2016).

*E-mail: matt@earth.northwestern.edu

One way to decipher the importance of increased volcanism and/or weathering rates on the sulfur cycle during this time is through the use of strontium (Sr) isotopes, because the geochemical cycles of S and Sr are linked through shared input fluxes of riverine (weathering) and hydrothermal inputs. The $^{87}Sr/^{86}Sr$ ratio of seawater represents a balance between hydrothermal (relatively unradiogenic, lower $^{87}Sr/^{86}Sr$) and terrestrial weathering (relatively radiogenic, higher $^{87}Sr/^{86}Sr$) inputs (Palmer and Edmond, 1989). While the relative ratio of these input fluxes largely controls the isotopic composition of the marine Sr reservoir, the output flux of pyrite burial exerts strong control over $\delta^{34}S_{sulfate}$ due to the large kinetic isotope effect associated with MSR and accompanying pyrite formation (Canfield and Teske, 1996). Thus, changes in the input fluxes (either in magnitude or isotopic composition) should be recorded in both isotope systems, while changes in the output flux (e.g., pyrite burial) should only affect the S cycle. If the Early Cretaceous negative S isotope shift was triggered by massive evaporite deposition and an attendant decrease in global pyrite burial rates, S and Sr isotope records should be decoupled. By contrast, if massive volcanism were responsible for driving the S isotope shift, one would expect a sympathetic shift in the $^{87}Sr/^{86}Sr$ ratio of seawater (as recorded in marine carbonate).

We present new S isotope data from Resolution Guyot, Mid-Pacific Mountains, that track sympathetically with Sr isotope records through the ~5‰ negative sulfur isotope shift, and employ a linked sulfur-strontium isotope mass-balance model to identify the mechanisms driving the sulfur isotope evolution of the Cretaceous ocean.

METHODS

Sulfur and Carbon Isotope Analysis

Carbonate-associated sulfate (CAS) was extracted by standard techniques (Hurtgen et al., 2006) and S isotope results are reported as per mil (‰) deviations from Vienna Canyon Diablo troilite (VCDT), using the conventional ($\delta^{34}S$) notation. Sulfur isotope results were reproducible within ±0.2‰, based on repeat analyses of standards. Carbon isotope results are reported as deviations (‰) from the carbon isotope composition of the Vienna Peedee belemnite (VPDB) standard and were reproducible within ±0.1‰ based on repeat analyses of standards. (See the GSA Data Repository[1] information for additional methods information.)

Coupled S-Sr Cycle Box Model

A box model was constructed to track the mass and isotopic composition of marine sulfate and Sr using the following equations:

$$\frac{dM_S}{dt} = hF_H^{Sr} + wF_W^{Sr} - F_{py}^S - F_{evap}^S, \quad (1)$$

and

$$\frac{dM_{Sr}}{dt} = F_H^{Sr} + F_W^{Sr} + F_D^{Sr} - \frac{M_{Sr}}{\tau_{Sr}}, \quad (2)$$

where M_S is the mass of sulfate in the ocean; M_{Sr} is the mass of Sr in the ocean; F_H^{Sr}, F_W^{Sr}, and F_D^{Sr} are the hydrothermal, weathering, and diagenetic input fluxes of Sr, respectively; h is the S/Sr ratio of the hydrothermal flux; w is the S/Sr ratio of the weathering flux; F_{py}^S and F_{evap}^S are the burial fluxes of pyrite and evaporite, respectively; and τ_{Sr} (constant) is the residence time of Sr in the ocean. The S and Sr isotope reservoirs are described by coupled isotope mass-balance equations:

$$\frac{dR_{SW}^S}{dt} = \frac{hF_H^{Sr}\left(R_H^S - R_{SW}^S\right) + wF_W^{Sr}\left(R_W^S - R_{SW}^S\right) - \Delta_{py}F_{py}}{M_S}, \quad (3)$$

and

$$\frac{dR_{SW}^{Sr}}{dt} = \frac{F_H^{Sr}\left(R_H^{Sr} - R_{SW}^{Sr}\right) + F_W^{Sr}\left(R_W^{Sr} - R_{SW}^{Sr}\right) + F_D^{Sr}\left(R_D^{Sr} - R_{SW}^{Sr}\right)}{M_{Sr}}, \quad (4)$$

where R_{SW}^S is the S isotope composition of seawater sulfate; R_{SW}^{Sr} is the $^{87}Sr/^{86}Sr$ ratio of seawater Sr; R_H^{Sr} and R_H^S are the Sr and S isotope composition of hydrothermal inputs, respectively; R_W^{Sr} and R_W^S are the Sr and S isotope composition of weathering inputs, respectively; R_D^{Sr} is the Sr isotope composition of the diagenetic input; Δ_{py} is the average isotope fractionation factor associated with pyrite deposition; and F_{py} is the burial flux of pyrite. The initial steady state for the Sr cycle was determined assuming that the magnitude of the hydrothermal flux and the $^{87}Sr/^{86}Sr$ ratios of the input fluxes (both hydrothermal and weathering) during the Early Cretaceous were comparable to the modern. The weathering flux was then calculated to achieve the observed pre-excursion R_{SW}^{Sr} (see the Data Repository for table detailing initial steady-state conditions). Steady state for the S cycle was determined by modifying the scaling parameters for the hydrothermal and weathering fluxes (h and w) using estimates for the modern S/Sr ratios of hydrothermal and weathering inputs (Palmer and Edmond, 1989; Arthur, 2000; Halevy et al., 2012). Furthermore, the model assumes an initial sulfate concentration of 6 mM (as opposed to modern levels of 28 mM), in accordance with Cretaceous estimates based on the chemical composition of fluid inclusions encased in halite (Lowenstein et al., 2001). The model also assumes that the relative ratios of S/Sr in hydrothermal and terrestrial weathering inputs have remained relatively constant over the past 130 m.y. Additional complexity was added to the model to explore the impact of a sulfate concentration-dependent pyrite burial term (see the Data Repository for discussion).

RESULTS

We extracted CAS from drill core collected at Resolution Guyot (Ocean Drilling Program [ODP] Site 866) to examine the relationship between $\delta^{34}S_{sulfate}$ and $\delta^{13}C_{carbonate}$ and previously published Sr isotope data (Jenkyns et al., 1995) from Early Cretaceous rocks. These data, plotted versus time (using the updated geological time scale of Ogg et al., 2012) in Figure 2 (see the Data Repository for age assignment details), indicate that while $\delta^{34}S_{sulfate}$ values are variable between ca. 130 and 126 Ma, there is a clear ~3‰ negative shift from an average of ~19‰ that stratigraphically correlates with the OAE1a positive $\delta^{13}C$ excursion. $\delta^{34}S_{sulfate}$ continues to fall after OAE1a for a total S isotope shift of ~4.5‰ before rebounding to pre-excursion values. The magnitude and timing of the $\delta^{34}S_{sulfate}$ negative shift are consistent with previously published $\delta^{34}S_{barite}$ data (Paytan et al., 2004). Importantly, the Sr isotope data (Jenkyns et al., 1995) shift sympathetically with $\delta^{34}S_{sulfate}$ and suggest that the geochemical cycles of S and Sr had roughly similar oceanic residence times and were at least partly coupled through this time period.

DISCUSSION

The Early Cretaceous record contains evidence for both extensive LIP volcanism and massive evaporite deposition; however, the relative timing of these events is critically important for the interpretation of the S and Sr isotope trends. A recent synthesis of the tectonic events associated with the breakup of South Africa and South America suggests that massive salt deposition in the South Atlantic basin occurred in the late Aptian (ca. 116–113 Ma; Chaboureau et al., 2013), whereas the major LIP events are thought to have occurred earlier. Mills et al. (2014) assigned the emplacement of the Ontong-Java and Manihiki Plateaus to the early Aptian (125 Ma) and the initiation of Kerguelen Plateau activity to 118 Ma.

Within this temporal context, we generated a coupled S-Sr box model to examine whether increases in hydrothermal activity, followed by massive evaporite deposition, are capable of reproducing the sympathetic shifts in $\delta^{34}S_{sulfate}$ and $^{87}Sr/^{86}Sr$ captured at Resolution Guyot. In the model we were able to reproduce the ~4.5‰ negative $\delta^{34}S_{sulfate}$ shift by simulating two periods of increased hydrothermal activity (scenario 1, Fig. 3): a
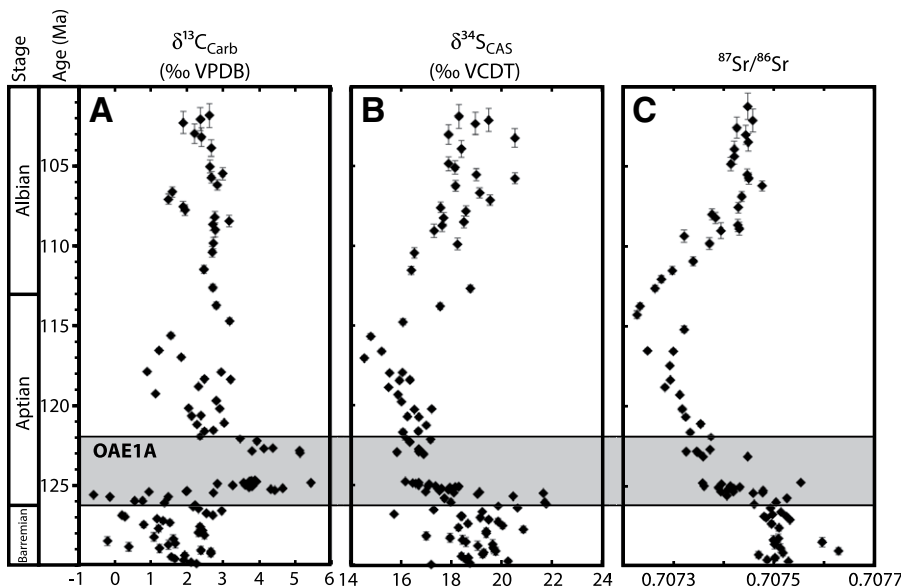
Figure 2. Geochemical results for rocks drilled at Resolution Guyot (Ocean Drilling Program Site 866) plotted versus time using data of Ogg et al. (2012). A: $\delta^{13}C_{carb}$ (VPDB, Vienna Peedee belemnite). B: $\delta^{34}S_{sulfate}$ (VCDT, Vienna Canyon Diablo troilite; CAS—carbonate-associated sulfate). C: $^{87}Sr/^{86}Sr$ (Jenkyns et al., 1995).

large, short time-scale increase in volcanic activity (8× increase for 0.5 m.y.) associated with the emplacement of the Ontong Java Plateau coincident with OAE1a, followed by a period of slightly elevated hydrothermal activity (1.7× hydrothermal flux) for 5.5 m.y.; and a second, smaller pulse of volcanism (2.3× hydrothermal flux for 5 m.y.), associated with the emplacement of the Kerguelen Plateau. The hydrothermal flux is maintained at 1.1× the original flux for the remainder of the simulation. While this elevated hydrothermal flux generates a $\delta^{34}S_{sulfate}$ shift similar in magnitude to that observed in the Resolution Guyot record, it produces unreasonably low $^{87}Sr/^{86}Sr$ ratios (blue line, Fig. 3A).

We were only able to reproduce the negative S and Sr isotope shifts recorded in Resolution Guyot rocks by increasing both hydrothermal and weathering fluxes (scenario 2, Fig. 3; see caption for flux increases). An important result of this model is that the negative S isotope shift is accompanied by a doubling of the marine sulfate reservoir (red line, Fig. 3C). If a period of increased evaporite deposition is added to the model corresponding to the late Aptian South Atlantic evaporite deposits (scenario 3, 6× increase in evaporite burial from 116 to 113 Ma; green line, Fig. 3), then the associated drawdown in marine sulfate concentration allows the

$\delta^{34}S_{sulfate}$ reservoir to rebound on a time scale similar to, or slightly faster than, the Sr isotope reservoir, as observed in the Resolution Guyot record (Fig. 2). This result only holds if pyrite burial rates are assumed to be independent of marine sulfate concentrations.

Although the timing of the $\delta^{34}S_{sulfate}$ negative shift recorded in CAS at Resolution Guyot is consistent with previously published $\delta^{34}S_{barite}$ data (Paytan et al., 2004), the return of $\delta^{34}S_{sulfate}$ to pre-excursion values occurs ~10 m.y. prior to the $\delta^{34}S_{barite}$ record. This discrepancy is not likely the result of temporal reconstruction errors, but rather indicates that this portion of the Resolution Guyot $\delta^{34}S_{CAS}$ record was influenced by either local environmental conditions and/or postburial alteration (see the Data Repository for more discussion). Given that the $\delta^{34}S_{barite}$ record was generated using multiple sections (Fig. 1), we assume it is more representative of global $\delta^{34}S_{sulfate}$ evolution during this time. Wortmann and Chernyavsky (2007) proposed that both the negative $\delta^{34}S_{sulfate}$ shift and the prolonged return to pre-excursion values resulted from evaporite burial; in their model, they prescribed a relationship between sulfate concentration and pyrite burial, where decreased sulfate concentrations (<10 mM) lead to decreased global pyrite burial rates. However, recent work suggests that
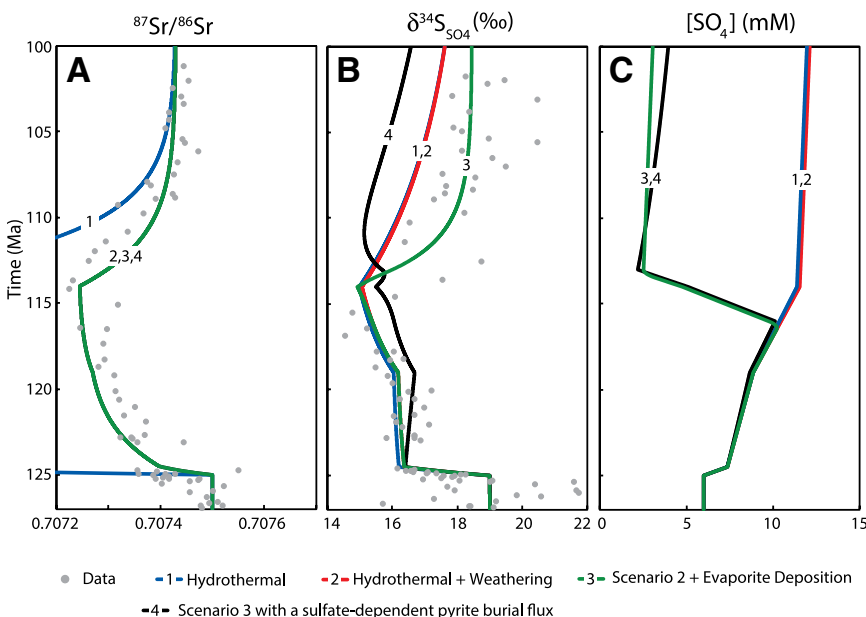

Figure 3. Modeled $^{87}Sr/^{86}Sr$, $\delta^{34}S_{sulfate}$, and sulfate concentration response to increased hydrothermal and weathering inputs and evaporite deposition. A: $^{87}Sr/^{86}Sr$. B: $\delta^{34}S_{sulfate}$ (‰). C: Sulfate concentration (mM). The models were forced as follows. 1: Hydrothermal increase only; an initial large pulse of volcanism (8× increase in hydrothermal flux for 0.5 m.y. at 125 Ma), followed by low-level volcanism (1.7× hydrothermal flux) for 5.5 m.y., followed by a second smaller pulse of volcanism (2.3× hydrothermal flux for 5 m.y.). The hydrothermal flux is then maintained at 1.1× the original flux for the remainder of the simulation. 2: The weather flux is increased alongside the hydrothermal flux: 4.2× hydrothermal + 3× weathering fluxes for 0.5 m.y.; 1.5× hydrothermal + 1.1× weathering for 5.5 m.y.; 1.8× hydrothermal + 1.3× weathering for 5 m.y.; 1.1× hydrothermal + 1× weathering for the remainder of the simulation. 3: Scenario 2, with an episode of evaporite deposition at 116 Ma (6× evaporite flux for 3 m.y.). 4: Scenario 3, using a sulfate concentration–dependent pyrite burial flux (see the Data Repository [see footnote 1] for discussion).

massive evaporite deposition occurred in the South Atlantic in the late Aptian, ~10 m.y. after the initiation of the negative S and Sr isotope shifts. Therefore, we propose that a simultaneous increase in the hydrothermal and weathering input fluxes associated with an increase in LIP volcanism best explains the coupled negative shift in the S and Sr isotope records. If we include massive evaporite deposition in our model during the late Aptian (9 m.y. after the initial onset of LIP volcanism) and assign a sulfate concentration-dependent pyrite burial flux (Wortmann and Chernyavsky, 2007; scenario 4, Fig. 3), the time scale of the $\delta^{34}S_{sulfate}$ rebound more closely matches the $\delta^{34}S_{barite}$ curve (Fig. 1; Paytan et al., 2004) and allows for marine sulfate concentrations to remain low for the interval leading up to OAE2 ca. 95 Ma (Wortmann and Chernyavsky, 2007; Adams et al., 2010; Owens et al., 2013; Gomes et al., 2016).

CONCLUSIONS

Our findings, in conjunction with recent temporal constraints for LIP emplacement and evaporite deposition during the Early Cretaceous, demonstrate that coupled increases in hydrothermal and weathering inputs, followed by a period of massive evaporite deposition, best explain the negative S and Sr isotope shifts recorded in rocks drilled at Resolution Guyot. This indicates that marine sulfate concentrations likely increased through most of the Aptian interval (including OAE1a) before dropping to lower levels via late Aptian evaporite deposition. Furthermore, the simultaneous increases in volcanism and weathering required to reconcile the S and Sr isotope records highlight the importance of feedback mechanisms in regulating atmospheric CO_2 levels (Berner et al., 1983; Kump et al., 2000). It has long been recognized that enhanced volcanism could increase atmospheric CO_2 concentrations and elevate weathering rates. However, in isolation, the marine Sr isotope record cannot be used to infer simultaneous increases (or decreases) in both hydrothermal and riverine fluxes. We propose the use of coupled S and Sr isotope measurements as a new tool for interpreting isotope records and identifying the processes that affect marine sulfate levels, and therefore the C cycle and the evolution of Earth's climate system, particularly during large-scale plate tectonic reorganization.

REFERENCES CITED
Adams, D.D., Hurtgen, M.T., and Sageman, B.B., 2010, Volcanic triggering of a biogeochemical cascade during Oceanic Anoxic Event 2: Nature Geoscience, v. 3, p. 201–204, doi:10.1038/ngeo743.

Arthur, M.A., 2000, Volcanic contributions to the carbon and sulfur geochemical cycles and global change, *in* Sigurdsson, B.F., et al., eds., Encyclopedia of volcanoes: San Diego, California, Academic Press, p. 1045–1056.

Berner, R.A., Lasaga, A.C., and Garrels, R.M., 1983, The carbonate-silicate geochemical cycle and its effect on atmospheric carbon dioxide over the past 100 million years: American Journal of Science, v. 283, p. 641–683, doi:10.2475/ajs.283.7.641.

Canfield, D.E., 2001, Isotope fractionation by natural populations of sulfate-reducing bacteria: Geochimica et Cosmochimica Acta, v. 65, p. 1117–1124, doi:10.1016/S0016-7037(00)00584-6.

Canfield, D.E., and Teske, A., 1996, Late Proterozoic rise in atmospheric oxygen concentration inferred from phylogenetic and sulphur-isotope studies: Nature, v. 382, p. 127–132, doi:10.1038/382127a0.

Chaboureau, A.-C., Guillocheau, F., Robin, C., Rohais, S., Moulin, M., and Aslanian, D., 2013, Paleogeographic evolution of the central segment of the South Atlantic during Early Cretaceous times: Paleotopographic and geodynamic implications: Tectonophysics, v. 604, p. 191–223, doi:10.1016/j.tecto.2012.08.025.

Chandler, M.T., Wessel, P., Taylor, B., Seton, M., Kim, S.-S., and Hyeong, K., 2012, Reconstructing Ontong Java Nui: Implications for Pacific absolute plate motion, hotspot drift and true polar wander: Earth and Planetary Science Letters, v. 331–332, p. 140–151, doi:10.1016/j.epsl.2012.03.017.

Davison, I., 2007, Geology and tectonics of the South Atlantic Brazilian salt basins, *in* Ries, A.C., et al., eds., Deformation of the continental crust: The legacy of Mike Coward: Geological Society of London Special Publication 272, p. 345–359, doi:10.1144/GSL.SP.2007.272.01.18.

Gomes, M.L., Hurtgen, M.T., and Sageman, B.B., 2016, Biogeochemical sulfur cycling during Cretaceous Ocean Anoxic Events: A comparison of OAE1a and OAE2: Paleoceanography, v. 31, p. 233–251, doi:10.1002/2015PA002869.

Halevy, I., Peters, S.E., and Fischer, W.W., 2012, Sulfate burial constraints on the Phanerozoic sulfur cycle: Science, v. 337, p. 331–334, doi:10.1126/science.1220224.

Hay, W.W., Migdisov, A., Balukhovsky, A.N., Wold, C.N., Fogel, S., and Soding, E., 2006, Evaporites and the salinity of the ocean during the Phanerozoic: Implications for climate, ocean circulation and life: Palaeogeography, Palaeoclimatology, Palaeoecology, v. 240, p. 3–46, doi:10.1016/j.palaeo.2006.03.044.

Hurtgen, M.T., Halverson, G.P., Arthur, M.A., and Hoffman, P.F., 2006, Sulfur cycling in the aftermath of a 635-Ma snowball glaciation: Evidence for a syn-glacial sulfidic deep ocean: Earth and Planetary Science Letters, v. 245, p. 551–570, doi:10.1016/j.epsl.2006.03.026.

Ingall, E.D., Bustin, R.M., and Van Cappellen, P., 1993, Influence of water column anoxia on the burial and preservation of carbon and phosphorus in marine shales: Geochimica et Cosmochimica Acta, v. 57, p. 303–316, doi:10.1016/0016-7037(93)90433-W.

Jenkyns, H.C., Paull, C.K., Cummins, D.I., and Fullagar, P.D., 1995, Strontium-isotope stratigraphy of lower Cretaceous atoll carbonates in the Mid-Pacific Mountains, *in* Winterer, E.L., et al., eds., Proceedings of the Ocean Drilling Program, Scientific results, Volume 143: College Station, Texas, Ocean Drilling Program, p. 89–97, doi:10.2973/odp.proc.sr.143.212.1995.

Jørgensen, B.B., 1982, Mineralization of organic matter in the sea bed—The role of sulphate reduction: Nature, v. 296, p. 643–645, doi:10.1038/296643a0.

Kump, L.R., Brantley, S.L., and Arthur, M.A., 2000, Chemical weathering, atmospheric CO_2, and climate: Annual Review of Earth and Planetary Sciences, v. 28, p. 611–667, doi:10.1146/annurev.earth.28.1.611.

Lowenstein, T.K., Timofeeff, M.N., Brennan, S.T., Hardie, L.A., and Demicco, R.V., 2001, Oscillations in Phanerozoic seawater chemistry: Evidence from fluid inclusions: Science, v. 294, p. 1086–1088, doi:10.1126/science.1064280.

Mills, B., Daines, S.J., and Lenton, T.M., 2014, Changing tectonic controls on the long-term carbon cycle from Mesozoic to present: Geochemistry, Geophysics, Geosystems, v. 15, p. 4866–4884, doi:10.1002/2014GC005530.

Ogg, J.G., Hinnov, L.A., and Huang, C., 2012, Cretaceous, *in* Gradstein, F.M., et al., eds., The geologic time scale 2012: Amsterdam, Elsevier, p. 793–853, doi:10.1016/B978-0-444-59425-9.00027-5.

Owens, J.D., Gill, B.C., Jenkyns, H.C., Bates, S.M., Seevermann, S., Kuypers, M.M.M., Woodfine, R.G., and Lyons, T.W., 2013, Sulfur isotopes track the global extent and dynamics of euxinia during Cretaceous Oceanic Anoxic Event 2: National Academy of Sciences Proceedings, v. 110, p. 18407–18412, doi:10.1073/pnas.1305304110.

Palmer, M.R., and Edmond, J.M., 1989, The strontium isotope budget of the modern ocean: Earth and Planetary Science Letters, v. 92, p. 11–26, doi:10.1016/0012-821X(89)90017-4.

Paytan, A., Kastner, M., Campbell, D., and Thiemens, M.H., 2004, Seawater sulfur isotope fluctuations in the Cretaceous: Science, v. 304, p. 1663–1665, doi:10.1126/science.1095258.

Prokoph, A., Shields, G.A., and Veizer, J., 2008, Compilation and time-series analysis of a marine carbonate $\delta^{18}O$, $\delta^{13}C$, $^{87}Sr/^{86}Sr$ and $\delta^{34}S$ database through Earth history: Earth-Science Reviews, v. 87, p. 113–133, doi:10.1016/j.earscirev.2007.12.003.

Schlanger, S.O., and Jenkyns, H.C., 1976, Cretaceous anoxic events: Causes and consequences: Geologie en Mijnbouw, v. 55, p. 179–184.

Van Cappellen, P., and Ingall, E.D., 1996, Redox stabilization of the atmosphere and oceans by phosphorus-limited marine productivity: Science, v. 271, p. 493–496, doi:10.1126/science.271.5248.493.

Wortmann, U.G., and Chernyavsky, B.M., 2007, Effect of evaporite deposition on Early Cretaceous carbon and sulphur cycling: Nature, v. 446, p. 654–656, doi:10.1038/nature05693.

Wortmann, U.G., and Paytan, A., 2012, Rapid variability of seawater chemistry over the past 130 million years: Science, v. 337, p. 334–336, doi:10.1126/science.1220656.

Zeebe, R.E., and Wolf-Gladrow, D.A., 2001, CO_2 in seawater: Equilibrium, kinetics, isotopes: Elsevier Oceanography Series Volume 65, 360 p.